

## Upscaling of Miscible Displacement Processes

*Sigurd í Jákupsstovu,<sup>1</sup> Dengen Zhou,<sup>2,\*</sup> Jairam Kamath,<sup>2</sup> Lou Durlofsky,<sup>3</sup> Erling H. Stenby<sup>1</sup>*  
<sup>1</sup>IVC-SEP, Technical University of Denmark, <sup>2</sup>Chevron Petroleum Technology Company, <sup>3</sup>Stanford University

### Abstract

In this paper, we present an approach for upscaling miscible displacement processes using a modified Todd-Longstaff (T-L) formulation. The T-L formulation is modified to include pseudo fractional flow curves. The pseudo fractional flow curves are calculated for each upscaled grid using the upscaling technique proposed by Christie *et al.*<sup>1</sup> The new procedure is applied to a 2-D cross-section model. We examined the effects of two commonly-used boundary conditions in the upscaling calculations.

Our preliminary results indicate that the generated pseudos are strong functions of the boundary conditions and how the average concentration is calculated. For the case we studied here, the pseudos generated using standard boundary conditions and volume averaged concentrations yield the best agreement with the fine scale simulations. The Effective Flux Boundary Conditions<sup>2,3</sup> tend to underestimate solvent production.

### Introduction

Gas injection becomes increasingly important for oil recovery and environmental considerations in oil field development. Gas injection processes are most effective when the injected gas is nearly or completely miscible with the oil in the reservoir. Commonly, water alternating gas (WAG) injection is employed to gain better profile control in a gas injection project. However, in some situations minimal water involvement is desired, and WAG is not applicable. In this paper we are concerned with a continuous miscible gas injection process in which water is immobile.

Theoretically one can simulate such processes with great accuracy if the grids are sufficiently fine. However, for field scale simulations, the required number of grids can be many orders of magnitude larger than what we can effectively handle with our current computation power. To bridge this gap of detail it is necessary to conserve the effective properties of the fine scale model to ensure that the coarse scale flow is representative of the actual system. The methodology for transferring the properties from a fine scale to a coarser scale is referred to as upscaling. The properties addressed for upscaling are both of static and dynamic nature. Static properties (permeability, porosity ..) can be upscaled through an averaging scheme or through single phase flow calculations while dynamic properties (fractional flow, total mobility ..) are upscaled through multi component flow calculations. Continuous miscible gas injection is commonly unstable because of the strong interaction of reservoir heterogeneity and unfavorable mobility ratios and therefore, appropriate upscaling of the dynamic properties becomes very important.

Todd-Longstaff<sup>4</sup> models are generally used for field scale miscible flood simulations. In simulating a fully miscible process, the mixing parameter,  $w$ , is the sole upscaling parameter.

---

\* To whom all correspondence shall be sent.

The value of  $\mathbf{w}$  is determined by matching the coarse grid simulations with fine grid simulations. The  $\mathbf{w}$  parameter has very limited upscaling capability. Fayers *et al.*<sup>5</sup> proposed to extend the T-L model with two omegas. In their method the omega factors for viscosity ( $\mathbf{w}_m$ ) and for density ( $\mathbf{w}_r$ ) are found using a matching technique against the fine grid reference results. They found that  $\mathbf{w}_m=0$  matches their fine grid simulations, suggesting that de-coupling of the viscosity and density calculations is not sufficient to increase the upscaling capability of the T-L model.

Christie *et al.*<sup>1</sup> proposed a renormalization-based method for upscaling miscible displacement processes, which is similar to Stone's<sup>6</sup> total mobility method for immiscible processes. The fractional flow curve and the effective hydrocarbon mobility are calculated for each upscaled cell. This method is legitimate for all range of miscible simulations, but require a new reservoir simulation formulation, because T-L models cannot use the fractional flow curves and effective hydrocarbon viscosity directly. Zhang and Sorbie<sup>7</sup> proposed a similar procedure for upscaling both immiscible and miscible gas displacement processes.

In this paper, we present a systematic approach where the Todd-Langstaff formulation is modified to include pseudo relative permeability curves calculated from the fractional flow and the total mobility.

## Miscible Formulations

### Todd-Longstaff (T-L) formulation

The miscible formulation was first proposed by Todd and Langstaff.<sup>4</sup> They defined effective properties as functions of the empirical parameters, omega,  $\mathbf{w}$ , and alfa,  $\mathbf{a}$ .  $\mathbf{w}$  reflects the effect of the porous media (heterogeneity) on the mixing of the fluids. For example a high permeability channel between an injector and producer would result in a poor mixing and yield low  $\mathbf{w}$  values.  $\mathbf{a}$  represents the miscibility of the solvent and oil when contacted.

The effective relative permeability,  $k_{re}$ , in the original T-L formulation is given by Eq. 1. For  $\mathbf{a}=1$ , the system is considered fully miscible and the component (oil or solvent) flow is governed by straight line relative permeability functions,  $k_{rm}$ . For  $\mathbf{a}=0$ , the system is considered immiscible and the component (oil or solvent) flow is governed by the immiscible relative permeability functions,  $k_{rim}$ . The effective relative permeability is a linear combination of  $k_{rm}$  and  $k_{rim}$ ,

$$k_{re} = (1 - \mathbf{a})k_{rim} + \mathbf{a}k_{rm} \quad (1)$$

The effective viscosity,  $\mu_{le}$ , is calculated by Eq. 2.  $\mu_{le}$  depends on  $\alpha$  as well as on  $\omega$ , and therefore the effective fluid properties and the effective relative permeability is coupled through  $\alpha$ ,

$$\mathbf{m}_{le} = \mathbf{m}_i^{(1-\mathbf{a}\omega)} \mathbf{m}_m^{\mathbf{a}\omega} \quad (i = \text{oil, solvent}) \quad (2)$$

The mixture viscosity  $\mathbf{m}_m$  is calculated from the quarter power law given in Eq. 3,

$$\frac{1}{\mathbf{m}_m^{1/4}} = \frac{c}{\mathbf{m}_s^{1/4}} + \frac{1-c}{\mathbf{m}_o^{1/4}} \quad (3)$$

where  $c$  is the solvent concentration.

When modeling fully miscible processes,  $\omega$  is the only up-scalable parameter in the original T-L formulation, as the relative permeability curves are straight lines.  $\omega$  has very limited up-scale capability for heterogeneous systems.

### *Modified T-L Formulation*

To capture the channeling effects in heterogeneous systems, we modified the T-L formulation to include pseudo-relative permeability curves (Zhou *et al.*<sup>8</sup>). For a fully miscible process, the modification is simple and straight-forward. We turned off the effective relative permeability calculations given by Eq. 1 which enables the simulator to use the pseudo relative permeability curves from the input deck. Thus, for coarse grid simulations we have two up-scalable parameters,  $\mathbf{w}$  and the pseudo relative permeability. We use  $\mathbf{w}$  to ensure the correct injectivity (effective viscosity) and the pseudos to obtain appropriate recovery behavior (correct fractional flow).

### **Upscaling Procedure for Fully Miscible Processes**

We focus on fully miscible processes because upscaling of immiscible processes is well established. The first step is to calculate the solvent fractional flow curve and effective hydrocarbon viscosity by performing fine grid simulations.<sup>2,3</sup> The pseudo relative permeability curves are calculated by ensuring a correct fractional flow and total mobility for the upscaled grid. The pseudo relative permeability curves can then be used as region specific curves in Chevron's Reservoir Simulator, CHEARS.  $\mathbf{w}$  is determined by assuming the total mobility to be controlled by the solvent viscosity at higher solvent concentrations.

### *Fine Grid Simulation*

The solvent fractional flow,  $f_s$ , is calculated at the outlet face of the simulation grid,

$$f_s = \frac{\sum q_s}{\sum q_t} \quad (q = \text{flux}, s = \text{solvent}, t = \text{total}) \quad (4)$$

We also calculate an effective hydrocarbon viscosity,  $\mu_{he}$ , at the outlet face,

$$\mathbf{m}_{he} = \frac{\sum k_x}{\sum k_x / \mathbf{m}_m} \quad (5)$$

In an up-scaled grid it is necessary to use the effective viscosity in order to obtain the correct pressure gradient in the coarsened grid.

*Boundary Conditions.* It is important to point out that the calculated fractional flow curves and the effective hydrocarbon viscosity depends strongly on the boundary conditions used for the simulations. In this study, we examined two commonly used boundary conditions, namely a standard boundary conditions<sup>3</sup> and the effective flux boundary conditions.<sup>3</sup> The standard boundary conditions are referred to as "renorm" boundary conditions in the paper by Wallstrom *et al.*<sup>3</sup>

When standard boundary conditions are used, a constant pressure gradient is applied at the inlet and a constant pressure at the outlet. These boundary conditions do not take into account the effect of the surrounding permeability field.

With the Effective Flux Boundary Conditions,<sup>2,3</sup> the flux through the sub grid is scaled by the background global flux. This means that when the permeability is smaller than the background permeability the flux scales with the permeability, and when the permeability is higher than the background permeability the flux is attenuated by the surroundings and saturates at a maximum value.

**Concentration Calculations.** As the displacement process is considered to be fully miscible we refer to the solvent *concentration* rather than *saturation*. The fractional flow and total mobility are functions of the solvent concentration and therefore very much dependent on how the average concentration is calculated.

The function properties are normally generated by averaging over the outlet face cells while the corresponding concentration value is found either by outlet cell face averaging or by averaging over the full volume of the sub grid block. The effect of this is illustrated in figure 1, where the fractional flow is given both for volume averaging and for outlet averaging. The volume averaging is frequently used as a means to compensate for numerical dispersion. We compare results from the two averaging methods.

Figure 1 shows examples of calculated fractional flow and effective hydrocarbon viscosity. The shape of the curves is a strong function of the boundary conditions and the concentration averaging scheme used.

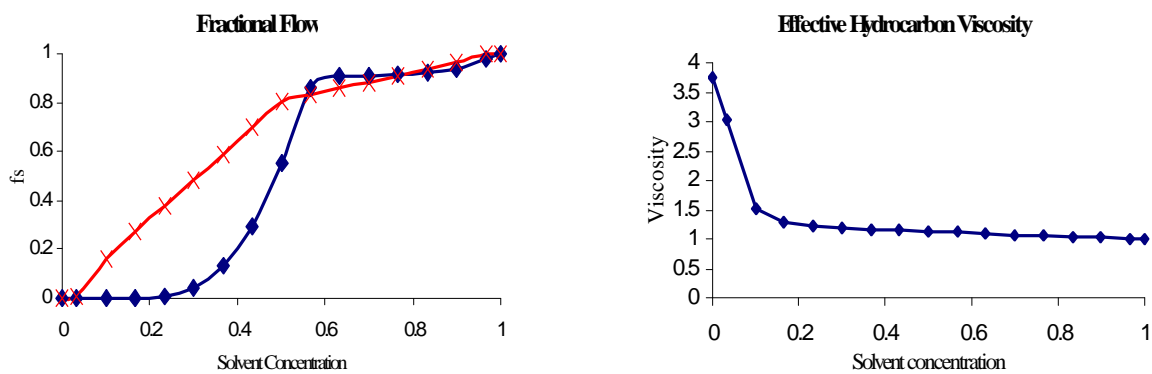


Fig. 1. Subgrid fractional flow and effective hydrocarbon viscosity. The fractional flow functions are given for concentrations averaged over the subgrid volume and for concentrations averaged over the outlet cells respectively. The viscosity function is given for concentrations averaged over the outlet cells.

### Coarse Grid Simulation

**Pseudo Relative Permeability.** On the coarse scale the solvent and oil flow is

$$q_l = \frac{\bar{k}k_{rl}}{\mathbf{m}_e} \nabla \bar{p} \quad (l = \text{oil, solvent, } \bar{k} = \text{effective permeability}) \quad (6)$$

The fractional flow for the coarsened grid can then be expressed by the following equation:

$$f_s = \frac{q_s}{q_s + q_o} = \frac{k_{rs} \mathbf{m}_{he}}{\mathbf{m}_{se}} \quad (7)$$

where  $k_{rs}$  is the solvent pseudo-relative permeability function.

Combining equations 2 and 7 yields

$$k_{rs} = \frac{f_s \mathbf{m}_{se}}{\mathbf{m}_{he}} = \frac{f_s \mathbf{m}_s^{1-w} \mathbf{m}_m^w}{\mathbf{m}_{he}} \quad (8)$$

$$k_{ro} = \frac{(1-f_s) \mathbf{m}_{oe}}{\mathbf{m}_{he}} = \frac{(1-f_s) \mathbf{m}_o^{1-w} \mathbf{m}_m^w}{\mathbf{m}_{he}} \quad (9)$$

As expected, the pseudo relative permeability equals to the fractional flow when omega is unity.

*Omega*,  $w$ . A value for  $w$  is needed in calculating the pseudos with equations 8 and 9. Because solvent is generally less viscous than the oil phase, the solvent viscosity dominates the total mobility of the system once solvent concentration reaches a certain level. We use  $m_{he} \approx m_{se}$  to estimate a value for  $\omega$  at high solvent concentrations. For highly heterogeneous systems,  $w$  is close to zero. Figure 2 is an example of estimating  $\omega$  from effective hydrocarbon viscosity.

Figure 3 gives examples of the calculated pseudo relative permeability curves. For this specific case, the pseudos indicate significant bypassing in this grid, which we would not be able to simulate using the original T-L model.

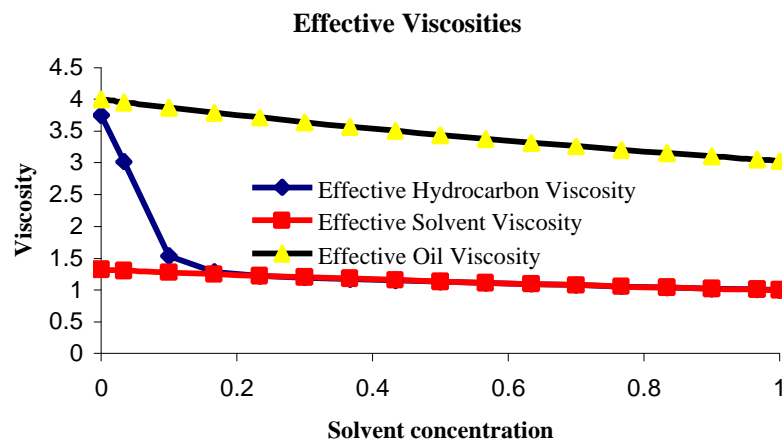


Fig. 2. Effective viscosity. It is seen that the effective hydrocarbon viscosity in this case is equal to the effective solvent viscosity for the majority of the saturation range.

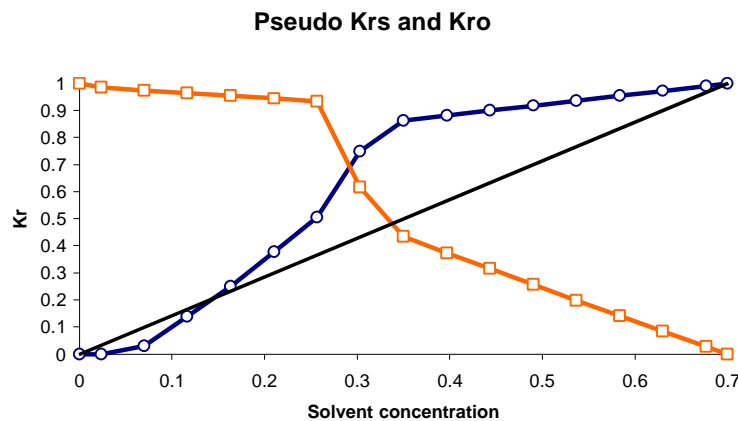


Fig. 3. Example of pseudo relative permeability curves. The shapes of the pseudos suggest substantial bypassing in this grid, comparing with straight line relative permeability curves used in original T-L model.

### Application to a 2-D Cross-section

As the first step, we tested the proposed procedure on a 2-D cross-section model where we have upscaled a 243x435 fine grid to 9x15 coarse grid. The fine grid reference simulations have been carried out using fully compositional simulations. The coarse grid simulations have been carried out using the modified miscible formulation and pseudo relative permeability curves as outlined above. As the simulator does not accommodate regional  $\omega$  factors at present, a global  $\omega$  parameter has been estimated for the coarse grid simulations.

### *Simulation results*

In Figure 4 a flow chart of the upscaling process is given. Local simulations are carried out sequentially for the chosen subdomains of the fine grid. From these simulations the coarse grid parameters and functions are calculated.

Four different coarse grid simulations are compared to the fine grid reference results. The VA-EFBC case uses the Effective flux boundary conditions and volume averaged concentrations. The VA-STBC results are obtained using volume averaged concentrations and standard boundary conditions. The OA-EFBC and OA-STBC results are obtained using outlet averaged concentrations with Effective flux boundary conditions and standard boundary conditions respectively.

The simulations are carried out specifying a maximum production rate and a minimum bottom hole producing pressure for the production well and a constant bottom hole injection pressure for the injector. The production time is 20 years.

In Figures 5 and 6 respectively the fine grid permeability field and the corresponding upscaled coarse grid permeability field are given. It is seen that the major features of the fine scale are captured in the coarser description.

In Figure 7 the coarse grid gas production using pseudo curves are compared to the fine grid results. It is seen that for the case presented here the standard boundary condition using volume averaged concentrations is reproducing the fine grid results very well. The effective flux boundary conditions tend to underestimate the solvent production both for volume and outlet averaged concentrations. For the OA-STBC case the solvent breaks through far too early.

In Figure 8 the average reservoir pressure for the coarse and fine scale simulations are presented. The results obtained using the standard boundary conditions and the volume averaged concentrations are the best match of the fine grid simulations.

Figure 9 shows the gas production rate vs cumulative gas injected. It is seen again that the results using standard boundary conditions and volume averaged concentrations reproduce the fine grid results closely.

In Figures 10 and 11 we show the solvent distributions from fine grid simulations and the coarse grid simulations using pseudos generated from standard boundary conditions and volume averaged solvent concentration after 5 years of production. The coarse grid simulation can reproduce the major features of the fine grid simulations.

### **Discussion**

The methodology presented here calculates pseudo relative permeability curves and omega using the fine grid information, and therefore no adjustable matching parameters are needed.

It was somewhat surprising that the best results were obtained using the standard boundary conditions, as previous work<sup>2,3</sup> find the effective flux boundary conditions to give the best results for two phase flow. We have not done any work on investigating the reasons for this. It is, however, suggested that one reason may be the very laminated permeability field with correlation lengths in excess of 50% in combination with an unfavorable mobility ratio (about 4). The effective flux boundary conditions are scaling local fluxes using a background-permeability. It is therefore likely that the attenuation imposed by effective flux boundary conditions is too high for this type of systems. Zhang and Sorbie<sup>7</sup> reported good matches of fine grid and coarse grid simulations using standard boundary conditions and volume averaged solvent concentration. The mobility ratios in Zhang and Sorbie's work were 3.85, 11.63 and 24.13. In future work we plan to further investigate the effect of using different boundary conditions and how the concentration sampling affects numerical dispersion and total mobility calculations.

## Conclusion

We have developed a procedure for upscaling miscible displacement processes using a modified Todd-Longstaff formulation. The Todd-Longstaff formulation has been modified to use grid block specific pseudo relative permeability curves for a fully miscible displacement process.

Our primary results suggest that in upscaling miscible processes one may need different boundary conditions from waterflood processes. More investigations are needed to quantify the differences in upscaling miscible gas and waterflood processes.

## Nomenclature

$f_s$	Solvent fractional flow
$f_o$	Oil fractional flow
$\mu_{he}$	Effective hydrocarbon viscosity
$\mu_s$	Solvent viscosity
$\mu_o$	Oil viscosity
$\mu_{oe}$	Effective oil viscosity
$\mu_{se}$	Effective solvent viscosity
$k_{rs}$	Solvent pseudo relative permeability
$k_{ro}$	Oil pseudo relative permeability
$\omega$	Omega factor
$\alpha$	Alfa factor
$q_t$	Total fluid flow rate
$q_s$	Solvent flow rate
$q_o$	Oil flow rate

## References

1. M.A. Christie, M. Mansfield, P.R. King, J.W. Barker and I.D. Culverwell: "A renormalization based upscaling technique for WAG floods in heterogeneous reservoirs," SPE29127, February 1995.
2. T.C. Wallstrom, M.A. Christie, L.J. Durlofsky, D.H. Sharp: "Effective flux boundary conditions for upscaling porous media equations," *Transport in Porous Media*, February 2002.
3. T.C. Wallstrom, S. Hou, M.A. Christie, L.J. Durlofsky, D.H. Sharp and Q. Zou: "Application of effective flux boundary conditions to two-phase upscaling in porous media," *Transport in Porous Media*, February 2002.
4. M.R. Todd and W.J. Langstaff: "The development, testing and application for a numerical simulator for predicting miscible performance," *JPT*, July 1972.
5. F.J. Fayers, H. Haajizadeh, C.Y. Lin, J. Taggart: "Use of the 4 component Todd and Langstaff method as an upscaling technique in simulating gas injection projects," SPE59340, 2000.
6. H.L. Stone: "Rigorous black oil pseudo functions," SPE21207, 1991.
7. H.R. Zhang, K.S. Sorbie: "The upscaling of miscible and immiscible displacement processes in porous media," SPE29931, 1995.
8. D. Zhou, C. Jensen, R. Tang and H. Arif: "A new formulation for simulating near miscible displacement processes," SPE56623, 1999.
9. J.R. Kyte, D.W. Berry: "New pseudo functions to control numerical dispersion," SPE5105, 1975.
10. K.H. Coats, J.R. Dempsey, J.H. Henderson: "The use of vertical equilibrium in two dimensional simulation of three dimensional reservoir performance," SPE2797, 1971.
11. J.W. Barker, F.J. Fayers: "Transport coefficients for compositional simulation with coarse grids in heterogeneous media," SPE22591, 1991.
12. J.W. Barker, S. Thibau, "A critical review of the use of pseudo relative permeabilities for upscaling," SPE35491, 1996.
13. M.R. Thiele, R.P. Batycky, M.J. Blunt and F.M. Orr: "Simulating flow in heterogeneous systems using streamtubes and streamlines," *SPE Reservoir Engineering*, February 1996.
14. M.A. Christie, P.J. Clifford: "Fast procedure for upscaling compositional simulation," SPE50992, 1998.

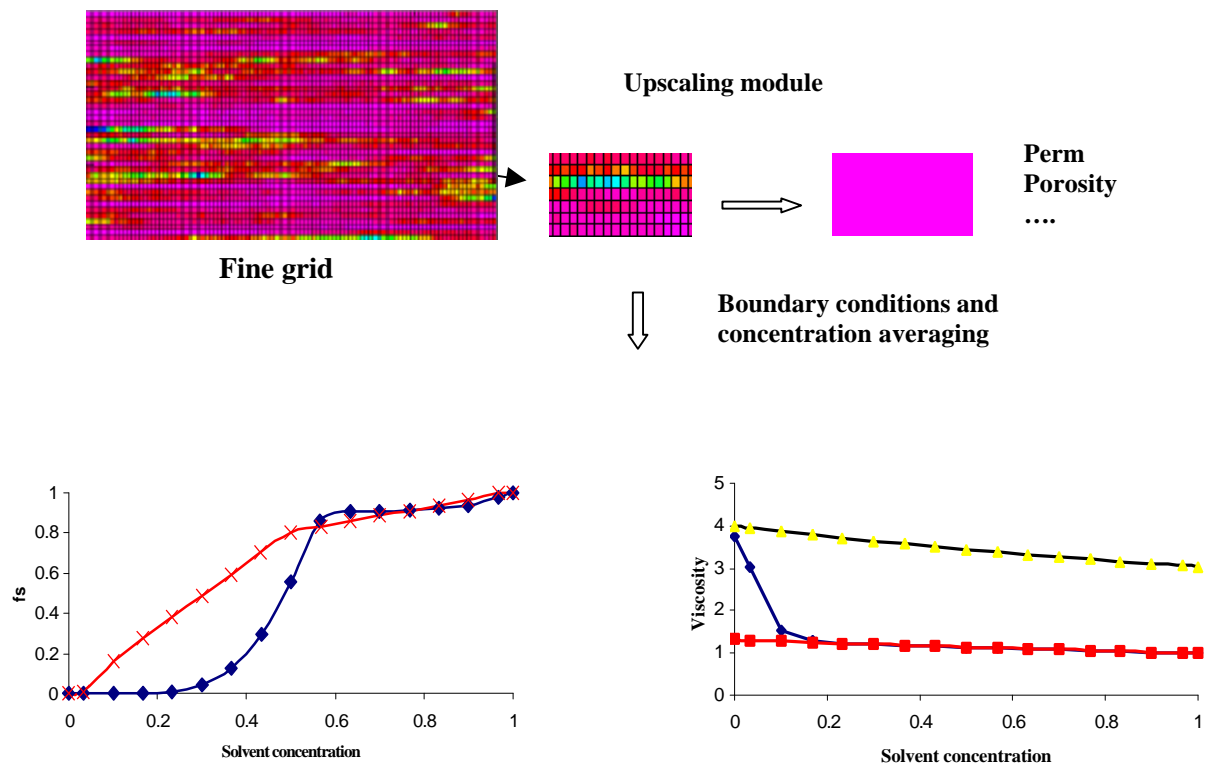


Fig. 4. Flow chart for the upscaling procedure. Local simulations are carried out for the subdomain of the fine grid. Based on these results static and dynamic properties are calculated. The upscaled dynamic properties obtained here is the phase fractional flow and the effective viscosity (total mobility). Based on these properties pseudo relative permeability curves and the mixing parameter  $w$  are calculated for each coarse grid block.

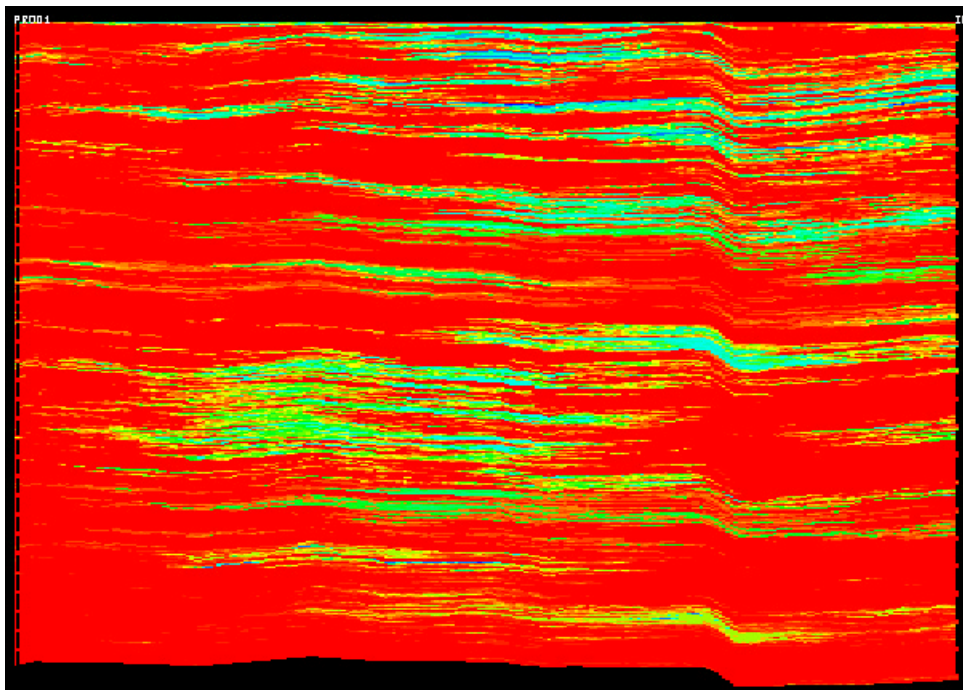


Fig. 5. Fine scale permeability field, 243 x 435 grid cells.

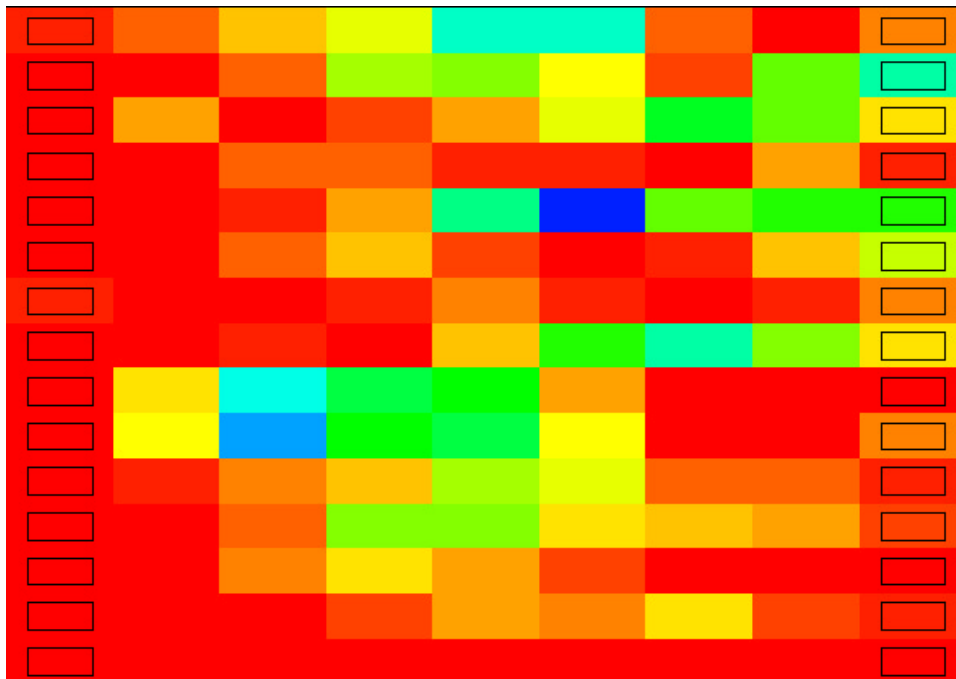


Fig.6. Coarse grid permeability field, 9 x 15 grid cells. The major features of the fine grid are seen to be captured by the coarse model.

### Solvent Production Rate

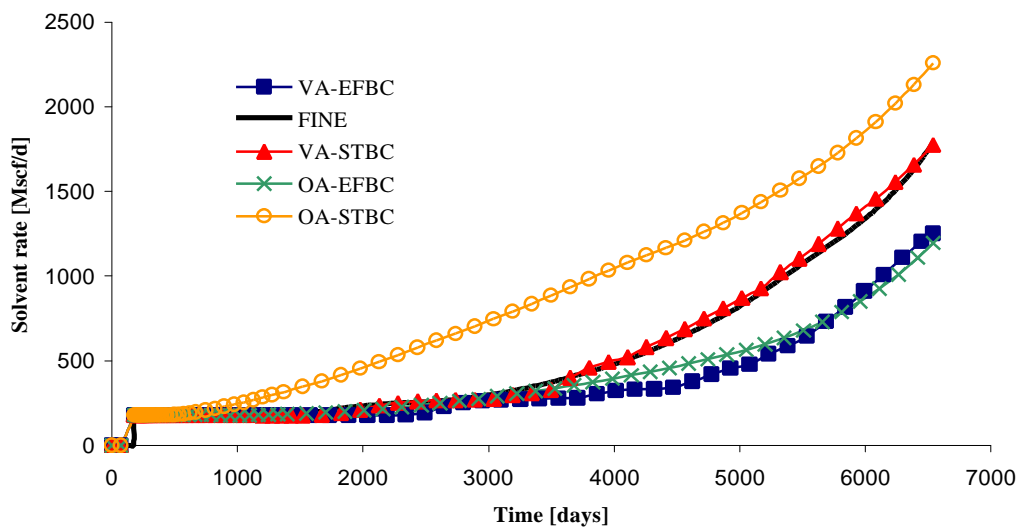


Fig. 7. Solvent production rate. The plot shows the results for 4 different coarse grid simulations compared to the fine grid reference results. The VA-EFBC case uses the Effective flux boundary conditions and volume averaged concentrations. The VA-STBC results are obtained using volume averaged concentrations and standard boundary conditions. The OA-EFBC and OA-STBC results are obtained using outlet averaged concentrations with Effective flux boundary conditions and standard boundary conditions respectively. It is seen that for the case presented here the standard boundary condition using volume averaged concentrations is reproducing the fine grid results very well. The Effective flux boundary conditions tend to underestimate the solvent production. For the OA-STBC case the solvent breaks through far to early.

The simulations are carried out specifying a maximum production rate and a minimum bottom hole producing pressure for the production well and a constant bottom hole injection pressure for the injector. The production time is 20 years.

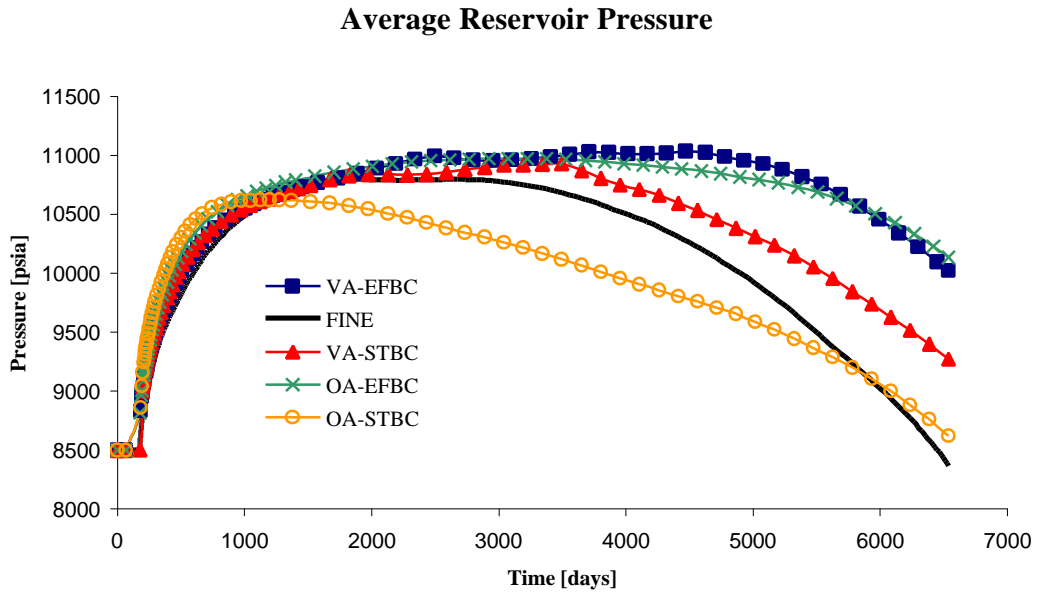


Fig. 8. Average reservoir pressure. The average reservoir pressure are compared for the 4 cases presented in this figure. The results obtained using the standard boundary conditions and the volume averaged concentrations give best results.

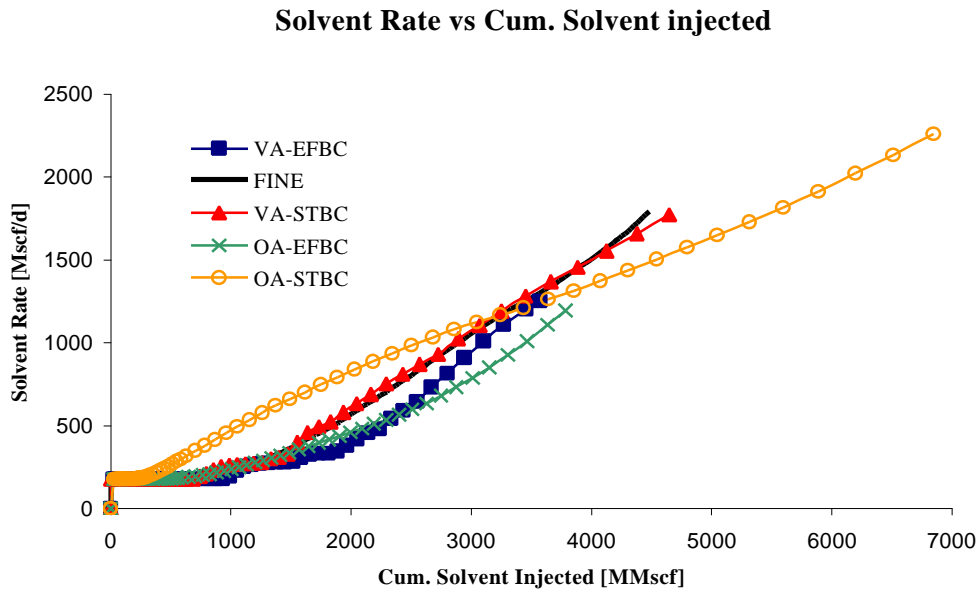


Fig. 9. Solvent production rate vs cumulative solvent injected. It is seen that the results using volume averaged concentrations and standard boundary conditions closely reproduces the fine scale results.

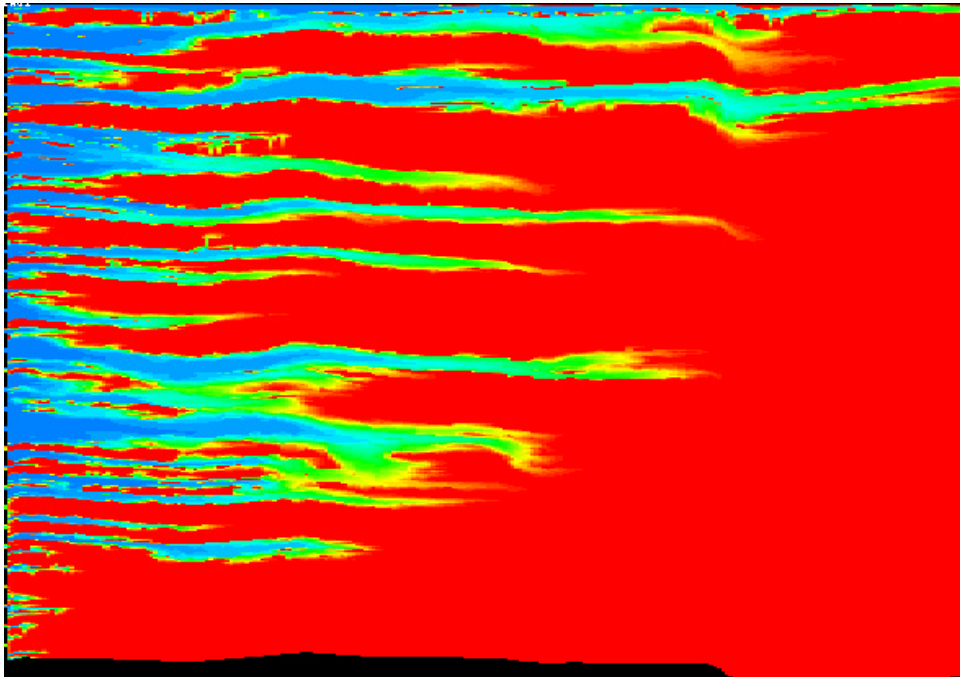


Fig. 10. Fine scale solvent concentration at 5 years production time.

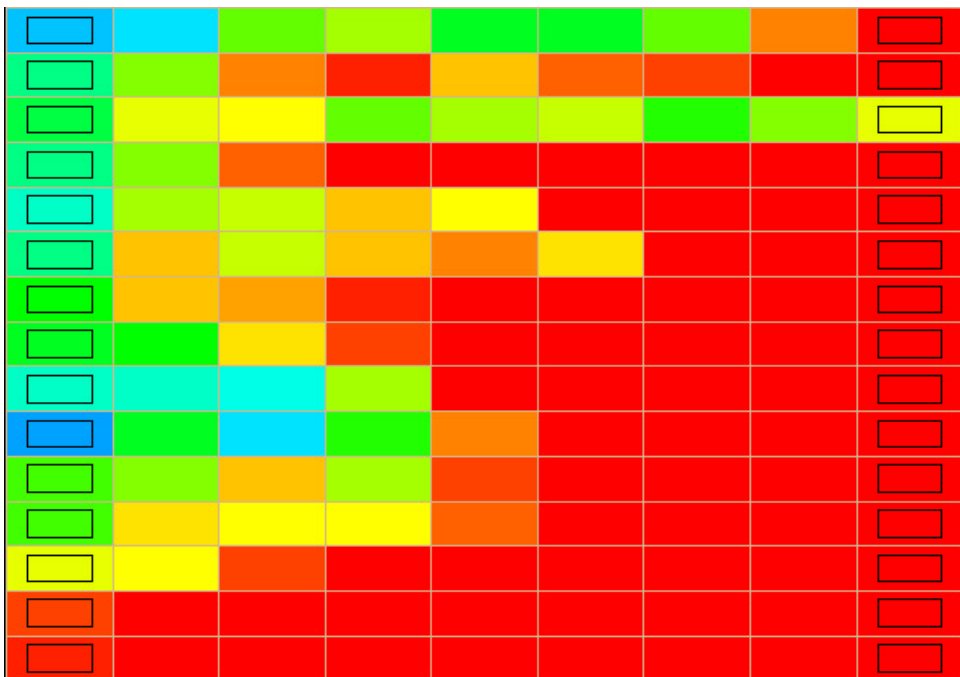


Fig. 11. Coarse scale solvent concentration at 5 years production time. The figure shows the solvent distribution for the coarse grid simulations using standard boundary conditions and volume averaged concentrations.